NONLINEAR EFFECTS IN CAVITATION CLOUD DYNAMICS

S. Kumar and C. E. Brennen
California Institute of Technology
Pasadena, California

Abstract

This paper presents a spectral analysis of the response of a fluid containing bubbles to the motions of a wall oscillating normal to itself. First, a fourier series analysis of the Rayleigh–Plesset equation is used to obtain an approximate solution for the nonlinear effects in the oscillations of a single bubble. This is used in the approximate solution of the oscillating wall problem and the resulting expressions are evaluated numerically in order to examine the nonlinear effects. The frequency content of the bubble radius and pressure oscillations near the wall is examined. Nonlinear effects are seen to increase with increased amplitude of wall oscillation, reduced void fraction and viscous and surface tension effects.

1. Introduction

The objective of this work is to gain an understanding of the interactions between individual bubbles in cavitating flows. The nonlinear dynamics of the growth and collapse of a single bubble have been studied for a long time (e.g. Plesset and Prosperetti (1977)). In a bubble cloud these nonlinear bubble dynamics produce nonlinear interactive effects. At most basic level, this interaction comes about because the response of the bubble to pressure changes results in volume changes which in turn cause accelerating velocity fields which effect the pressure. The present paper attempts to construct an approximate nonlinear analysis of this phenomenon.

Among the first to focus on the dynamics of bubble clusters was van Wijngaarden (1964) who analyzed the collapse of a large number of bubbles next to a flat wall and found considerable increase of pressure at the wall as result of the interactive effects. Morch (1980 and 1982), Hansson *et al.* (1982), Chahine (1982) and Omta (1987) have worked on other aspects of the dynamics of the bubble clouds. d'Agostino *et al.* (1988) solved for the linearized dynamics of the flow of bubbly mixture over over slender surfaces. d'Agostino and Brennen (1989) calculated natural frequencies of the bubble cloud and solved for linearized dynamics of spherical bubble clouds .

Apart from Omta's (1987) numerical solutions very little work has been done on the nonlinear dynamics of bubble clouds. The objective of present work is develop a methodology for handling nonlinear terms and to obtain the nonlinear solution in one illustrative case by studying the dynamics of bubbly liquid next to a flat wall which oscillates normal to its own plane. Only an abbreviated form of our work is presented here; details work will be presented elsewhere (Kumar and Brennen (1990)).

2. Notation

i	imaginary number
k	polytropic constant for gas expansion and contraction
j, n	index integer

p	pressure in liquid flow field
P_{go}	pressure of permanent gas in the bubble at undisturbed condition
P_n	complex amplitude of pressure oscillation at frequency $n\delta$
P_o	reference pressure in the liquid
P_v	vapor pressure inside the bubble
P_∞	pressure at infinity
R	radius of the bubble
R_o	radius of the bubble in reference condition
R_n	complex amplitude of radius oscillation at frequency $n\delta$
S	surface tension of the liquid
t	time
T	Lagrangian time
u	velocity in the liquid flow field
x	Eulerian space coordinate normal to the wall
X	Lagrangian space coordinate normal to the wall
X_n	complex amplitude of wall oscillation at frequency $n\delta$
α_o	volume fraction of bubbly mixture at reference condition
δ	increment in the frequency
γ	ratio of specific heats
ν	kinematic viscosity
ω_b	natural frequency of the bubble in radians/sec
ω_x	frequency of the wall oscillation in radians/sec
$\Re$	real part of complex quantity
τ	volume of the bubble
τ_n	complex amplitude of the bubble volume oscillation at frequency $n\delta$
τ_o	volume of the bubble at undisturbed condition
ρ	density of the liquid
ρ_v	density of the vapor in the bubble

3. Nonlinear Solution of the Rayleigh–Plesset Equation

There exists a substantial body of literature on the nonlinear dynamics of single bubbles (for example Eller and Flynn (1969), Prosperetti (1974) and Lauterborn (1976)); this has been reviewed by Plesset and Prosperetti (1977). In the present work it is necessary to construct the very simplest nonlinear solution of the Rayleigh–Plesset equation for a single bubble. Later this will be used as a building block for the problem of many bubbles interacting in a flow. The bubble is assumed to be spherical and to contain water vapor and residual permanent gas. The bubble interior is assumed to be uniform with constant vapor pressure, P_v. The permanent gas in the bubble is assumed to behave polytropically with an index k between 1 and γ(Plesset and Hsieh (1960)). The liquid compressibility is only included in the radiation damping which is accounted for by including it in effective viscosity in the bubble dynamics in the manner previously described by Devin (1959). With these assumptions the Rayleigh–Plesset equation describing the bubble dynamics becomes

$$R\frac{D^2R}{Dt^2}+\frac{3}{2}\left(\frac{DR}{Dt}\right)^2+\frac{4\nu}{R}\frac{DR}{Dt}+\frac{2S}{\rho R}=\frac{P_v(T_\infty)-P_\infty(t)}{\rho}+\frac{P_{go}}{\rho}\left(\frac{R_o}{R}\right)^{3k} \quad (1)$$

In the present solution a fourier series expansion method is used and terms up to second order are retained in order to examine these corrections to the linear solution. The bubble radius, $R(t)$ and the pressure at infinity, $P_\infty(t)$ are expanded in the form

$$R=R_o+\sum_{n=1}^{N}\Re\left(R_n e^{in\delta t}\right) \quad (2)$$

and

$$\frac{P_\infty(t)}{\rho}=P_o+\sum_{n=1}^{N}\Re\left(P_n e^{in\delta t}\right) \quad (3)$$

where P_n and R_n are complex quantities and $n\delta, n=1,N$ represents the discretization of the frequency domain. These are substituted into equation (1) and all terms of third or higher order in R_n/R_o are neglected in order to extract the simplest nonlinear effects. Finally, coefficients of $e^{in\delta t}$ on both sides of the simplified equation are equated. This yields following equation for P_n and R_n.

$$\frac{P_n}{\omega_b{}^2R_o{}^2}=\Lambda\frac{R_n}{R_o}+\sum_{j=1}^{n-1}\beta_1(n,j)\frac{R_j}{R_o}\frac{R_{n-j}}{R_o}+\sum_{j=1}^{N-n}\beta_2(n,j)\frac{\overline{R}_j}{R_o}\frac{R_{n+j}}{R_o} \quad (4)$$

where the bubble natural frequency, ω_b is given by $\omega_b=\left(3kP_{g0}/\rho R_o{}^2-2S/\rho R_o{}^3\right)^{1/2}$ and Λ, $\beta_1(n,j)$ and $\beta_2(n,j)$ are known complex coefficients defined by

$$\Lambda = \frac{n^2\delta^2}{{\omega_b}^2} - 1 - i\frac{n\delta}{\omega_b}\frac{4\nu}{\omega_b {R_o}^2} \tag{5}$$

$$\beta_1(n,j) = \frac{3k+1}{4} + \frac{3k-1}{2}\frac{S}{\rho{\omega_b}^2{R_o}^3} + \frac{1}{2}\frac{\delta^2}{{\omega_b}^2}(n-j)\left(n+\frac{j}{2}\right) + i\frac{2\nu}{\omega_b {R_o}^2}\frac{\delta}{\omega_b}(n-j) \tag{6}$$

$$\beta_2(n,j) = \frac{3k+1}{2} + (3k-1)\frac{S}{\rho{\omega_b}^2{R_o}^3} + \frac{1}{2}\frac{\delta^2}{{\omega_b}^2}\left(n^2 - nj - j^2\right) + i\frac{2\nu}{\omega_b {R_o}^2}\frac{n\delta}{\omega_b} \tag{7}$$

Note that the pressure perturbations, P_n occur in above analysis only in linear form and thus can be large without introducing error in the solution. However, the analysis is valid only for $R_n/R_o \ll 1$. This defines the extent of the weak nonlinear effects which are examined here and indirectly implies an upper limit on the magnitude of $P_n/{\omega_b}^2{R_o}^2$. These solutions were compared with numerical solutions of the complete Rayleigh–Plesset equation and were found to work well in predicting the amplitude of R_n/R_o (Kumar and Brennen (1990)). Obviously, more accurate nonlinear solutions than the one described above exist and have been expounded in the literature. The value of present solution lies in its simplicity and the feasibility of incorporating it in an analysis of the collective response of a cloud of bubbles.

4. Nonlinear flat wall solution

The specific problem addressed in this paper is shown schematically in Figure 1. Liquid containing bubbles is bounded by a flat wall which oscillates in a direction normal to itself at a given frequency, ω_x. The resulting flow is assumed to be function only of x and t. The approximations and assumptions involved in the solution of this problem are the same as those employed in the earlier work of d'Agostino *et al.* (1988) and d'Agostino and Brennen (1989). The bubbles are each assumed to be governed by the Rayleigh–Plesset equation (1) involving the local pressure $p(x,t)$ and the mixture is assumed to follow space averaged continuity and momentum equations. The solution to this problem is obtained in Lagrangian coordinates, X and T. Consistent with the structure of the solution

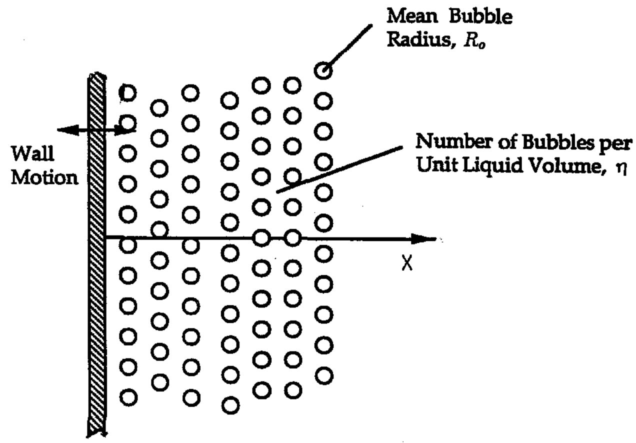

Figure 1: Schematic of the Oscillating Wall Problem.

sought, the relationship between Lagrangian and Eulerian coordinates, X and x, is written in the form

$$x = X + \sum_{n=1}^{N} \Re\left(X_n(X)e^{in\delta T}\right) \tag{8}$$

and the bubble volume, τ, and pressure, P, are expressed by the expansions

$$\tau = \tau_o + \sum_{n=1}^{N} \Re\left(\tau_n(X)e^{in\delta T}\right) \tag{9}$$

and

$$\frac{P}{\rho} = P_o + \sum_{n=1}^{N} \Re\left(P_n(X)e^{in\delta T}\right) \tag{10}$$

These are substituted into governing equations and coefficients of $e^{in\delta T}$ are equated. After simplification we obtain

$$\frac{d^2\left(P_n/{\omega_b}^2{R_o}^2\right)}{d(x/R_o)^2} = 3\alpha_o(1-\alpha_o)\left(\frac{n\delta}{\omega_b}\right)^2\frac{R_n}{R_o} + f_{n1}(X) \tag{11}$$

where $f_{n1}(X)$ is defined by

$$f_{n1}(X) = 3\alpha_o(1-\alpha_o)\left(\frac{n\delta}{\omega_b}\right)^2\left[\sum_{j=1}^{n-1}\left(\frac{1}{2} + \frac{3\alpha_o(2j-n)}{2n}\right)\cdot\frac{R_j}{R_o}\frac{R_{n-j}}{R_o} + \sum_{j=1}^{N-n}\frac{\overline{R_j}}{R_o}\frac{R_{n+j}}{R_o}\right] \tag{12}$$

The two equations (4) and (11) which connect $P_n(X)$ and $R_n(X)$ may be solved (see Kumar and Brennen (1989)) to yield the following implicit relation between the coefficients.

$$-\frac{\lambda_n}{3\alpha_o}\frac{X_n(0)}{R_o} = S_n + \sum_{j=1}^{n-1}\beta_5(n,j)\,S_jS_{n-j} + \sum_{j=1}^{N-n}\beta_6(n,j)\,\overline{S_j}S_{n+j} \tag{13}$$

where $X_n(0)/R_o$ is the ratio for the wall amplitude to the mean bubble radius. Here λ_n, $\beta_5(n,j)$, $\beta_6(n,j)$ are defined as

$$\lambda_n^2 = 3\alpha_o(1-\alpha_o)\left(\frac{n\delta}{\omega_b}\right)^2/\Lambda \tag{14}$$

$$\beta_5(n,j) = \frac{\lambda_n(\lambda_j+\lambda_{n-j})}{(\lambda_j+\lambda_{n-j})^2-\lambda_n^2}\begin{bmatrix}\frac{1}{2}+3\alpha_o\frac{(2j-n)}{2n}\\ -\beta_1(n,j)/\Lambda\end{bmatrix} \tag{15}$$

$$\beta_6(n,j) = \frac{\lambda_n\left(\overline{\lambda_j}+\lambda_{n+j}\right)}{\left(\overline{\lambda_j}+\lambda_{n+j}\right)^2-\lambda_n^2}\left[1-\beta_2(n,j)/\Lambda\right] \tag{16}$$

The radius coefficient functions, $R_n(X)/R_o$ are given by

$$\frac{R_n}{R_o} = \left[Q_n e^{-\lambda_n X/R_o} + f_{n3}(X) - f_{n2}(X)\right]/\Lambda \tag{17}$$

and the pressure coefficient functions, $P_n(X)/\omega_b^2R_o^2$ are given by

$$\frac{P_n}{\omega_b^2R_o^2} = Q_n e^{-\lambda_n X/R_o} + f_{n3}(X) \tag{18}$$

where

$$f_{n2}(X) = \sum_{j=1}^{n-1}\beta_1(n,j)\frac{R_j}{R_o}\frac{R_{n-j}}{R_o} + \sum_{j=1}^{N-n}\beta_2(n,j)\frac{\overline{R_j}}{R_o}\frac{R_{n+j}}{R_o} \tag{19}$$

$$f_{n3}(X) = \begin{bmatrix}\sum_{j=1}^{n-1}\beta_3(n,j)\,S_jS_{n-j}e^{-(\lambda_j+\lambda_{n-j})X/R_o}\\ +\sum_{j=1}^{N-n}\beta_4(n,j)\,\overline{S_j}S_{n+j}e^{-(\overline{\lambda_j}+\lambda_{n+j})X/R_o}\end{bmatrix} \tag{20}$$

$$Q_n = S_n\Lambda \tag{21}$$

$$\beta_3(n,j) = \frac{\lambda_n^2}{(\lambda_j+\lambda_{n-j})^2-\lambda_n^2}\begin{bmatrix}\Lambda\left(\frac{1}{2}+3\alpha_o\frac{(2j-n)}{2n}\right)\\ -\beta_1(n,j)\end{bmatrix} \tag{22}$$

$$\beta_4(n,j) = \frac{\lambda_n^2}{\left(\overline{\lambda_j}+\lambda_{n+j}\right)^2-\lambda_n^2}\left[\Lambda-\beta_2(n,j)\right] \tag{23}$$

This completes the solution for a given fluid and given bubble properties.

5. Results and Discussion

For a given wall amplitude to bubble radius ratio, $X_n(0)/R_o$ and given bubble properties the equation (13) is solved for S_n (or R_n/R_o at the wall) using a Newton–Raphson procedure. Then $P_n/\omega_b^2R_o^2$ at the wall is calculated using equation (18).

Table 1: Fluid and Bubble Parameters for the examples presented. These data are for water at 20° C

Data Set	R_o (μm)	P_{go} (Pa)	k	$\nu/\omega_bR_o^2$	$S/\rho\omega_b^2R_o^3$
I	20	14680	1	0.01	0.10
II	20	106326	1	0.0028	0.0118

It is obvious from an examination of the structure of equations that the results are independent of the way the frequency domain is discretized, or in other words the parameter δ. Also, it is seen from the computation that both $P_n/\omega_b^2R_o^2$ and R_n/R_o appear only at harmonics of the frequency of the wall oscillation, ω_x. Thus the software may be written so as to evaluate only the harmonics of nonzero amplitude. For the purpose of demonstrating the nonlinear effects, we choose to vary the wall oscillation frequency from $\omega_b/100$ to $2\omega_b$ and the resulting magnitudes of the harmonics $P_n/\omega_b^2R_o^2$ and R_n/R_o at the wall are plotted as functions of the nondimensionalized frequency $n\delta/\omega_b$. Data for the two sets of values of the viscous parameter, $\nu/\omega_bR_o^2$ and the surface tension parameter, $S/\rho\omega_b^2R_o^3$ listed in Table 1 will be presented. Data set I provides a convenient reference case in which, in addition the mean void fraction, α_o is taken to be 0.02 and the amplitude of wall oscillation, $X_n(0)/R_o$ is taken to be 0.03. Data set II is used to examine the effect of varying the viscous and surface tension parameters. The effects of varying α_o and $X_n(0)/R_o$ on the results will also be examined.

Results for the reference case are presented in Figure 2. The lines labelled [1] are the magnitudes of the response at the fundamental forcing frequency so that, in this case, the abscissa represents ω_x/ω_b. The lines labelled [2] represent the magnitudes of the response at twice the forcing frequency; and in this case abscissa, represents $2\omega_x/\omega_b$. And so on for the lines labelled [3], [4] and [5] which represent the response at the third, fourth and fifth harmonics of the forcing frequency. For all the lines magnitudes are plotted against the actual reduced frequency, ω/ω_b, at which they occur. In this figure we

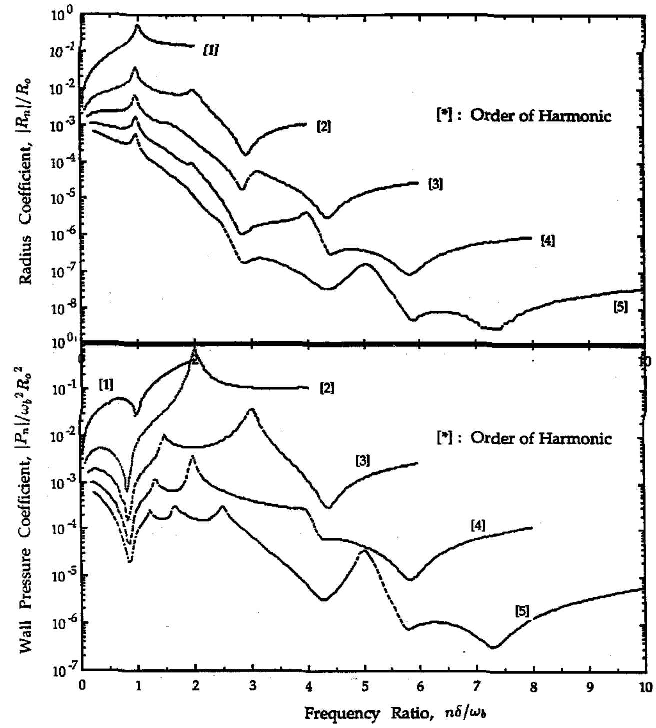

Figure 2: The frequency response of the bubbly cloud; $|R_n|/R_o$ and $|P_n|/\omega_b{}^2R_o{}^2$ are plotted against the frequency ratio, $n\delta/\omega_b$ for the first five harmonics. The parameters: $X_n(0)/R_o = 0.03$, α_o= 0.02 and $\nu/\omega_b R_o{}^2$ and $S/\rho\omega_b{}^2 R_o{}^3$ are as in data set I.

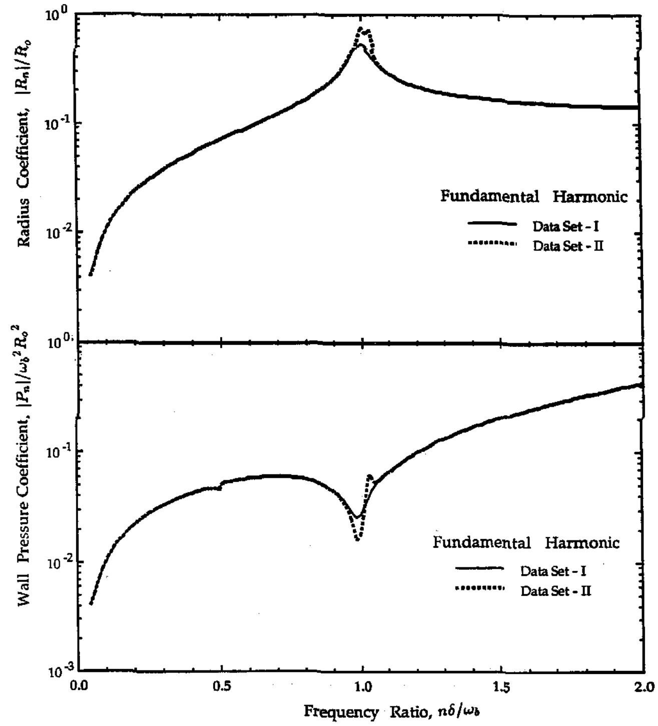

Figure 3: The effect of variation in $\nu/\omega_b R_o{}^2$ and $S/\rho\omega_b{}^2 R_o{}^3$ on the fundamental harmonic; $|R_n|/R_o$ and $|P_n|/\omega_b{}^2R_o{}^2$ for the fundamental harmonic are plotted against the frequency ratio, $n\delta/\omega_b$. The parameters: $X_n(0)/R_o = 0.03$, α_o= 0.02 and $\nu/\omega_b R_o{}^2$ and $S/\rho\omega_b{}^2 R_o{}^3$ are as in data sets I and II.

have presented the results for harmonics up to fifth order. In viewing these results it should be recognised that those harmonics with magnitudes below a certain level are of dubious significance since higher order nonlinearities would, in all likelihood, markedly alter those results.

The first point to note is that the response rapidly decays at higher harmonics. For the purpose of discussion of the results a frequency at which the response is a maximum will be called an enhancement frequency and a frequency at which the response is a minimum will be called a suppression frequency. From the Figure 2, it can be seen that the dominant enhancement frequency for bubble radius oscillations at the wall is ω_b. Furthermore, harmonics of all orders have a *suppression frequency of approximately $3\omega_b$ though the reasons* for this are not clear. It can also be seen that the higher harmonics of radius oscillations have other enhancement and suppression frequencies.

In contrast to the radius oscillations, all of the harmonics of the pressure have suppression frequencies close to ω_b. The suppression in the fundamental harmonic at ω_b is also predicted by the linear solution. It can be seen that the dominant second harmonic occurs at approximately $2\omega_b$ and the dominant third harmonic at approximately $3\omega_b$. The fundamental in the pressure oscillation reaches a minimum at approximately ω_b and then increases linearly with frequency. Thus the pressure response is dominated by the fundamental and the second harmonic at $2\omega_b$. High pressure response at the second harmonic is the main result obtained from nonlinear analysis. This can be explained as follows. When the wall is oscillated close to ω_b the bubble volume response is sufficiently large to cause significant accelerations in the fluid. Thus high pressure fluctuations can be expected. This takes the form of a substantial pressure oscillation at the second harmonic, $2\omega_b$.

The effect of changing the viscous and the surface tension parameters while all other parameters remain unchanged is illustrated in Figure 3 which presents a comparison between the results for the data set II and the earlier results for the

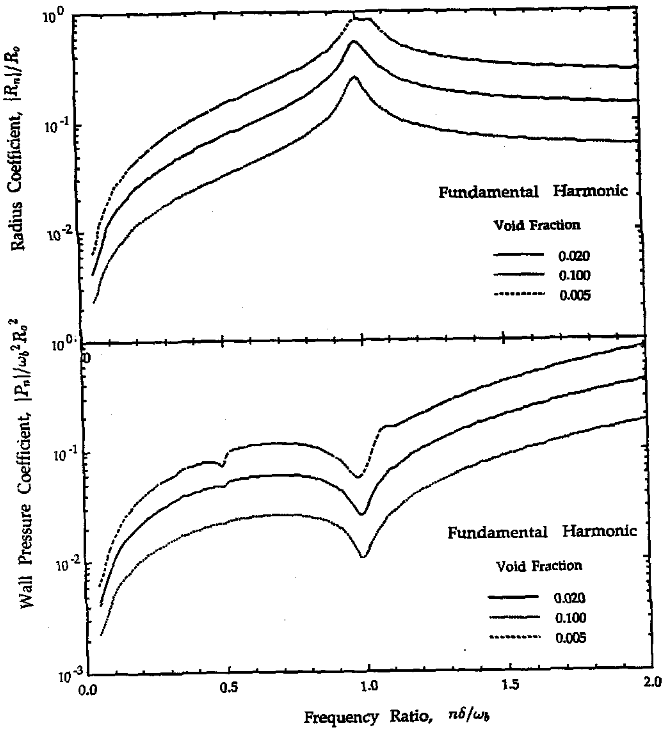

Figure 4: The effect of change in the void fraction, α_o on the fundamental harmonic; $|R_n|/R_o$ and $|P_n|/\omega_b{}^2 R_o{}^2$ for the fundamental harmonic are plotted against the frequency ratio, $n\delta/\omega_b$. The parameters: $X_n(0)/R_o = 0.03$ and $\nu/\omega_b R_o{}^2$ and $S/\rho\omega_b{}^2 R_o{}^3$ values are as in data set I. Values of the void fraction, α_o, of 0.005, 0.020 and 0.100 are used.

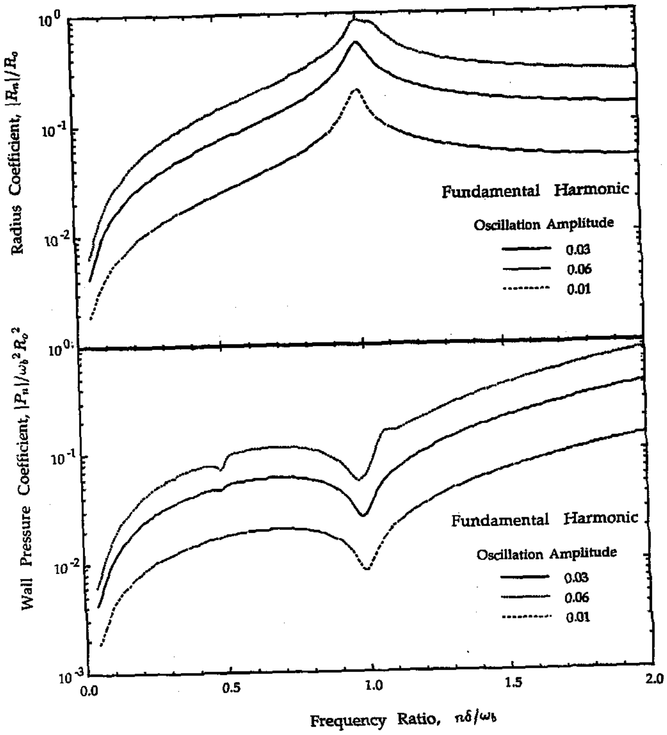

Figure 5: The effect of change in the amplitude of wall oscillation, $X_n(0)/R_o$ on the fundamental harmonic; $|R_n|/R_o$ and $|P_n|/\omega_b{}^2 R_o{}^2$ for the fundamental harmonic are plotted against the frequency ratio, $n\delta/\omega_b$. The parameters: $\alpha_o = 0.02$ and $\nu/\omega_b R_o{}^2$ and $S/\rho\omega_b{}^2 R_o{}^3$ values are as in data set I. $X_n(0)/R_o$ values of 0.01, 0.03 and 0.06 are used.

data set I. Higher viscous and surface tension parameters tend to inhibit the bubble oscillations. Hence the results for the data set II exhibit sharper peaks and troughs in the response curves. Otherwise the basic form of the response is very similar for the two sets of data with only minor differences in enhancement and suppression frequencies due to differences in the levels of nonlinearity. Two additional features of the results presented in Figure 3 deserve special attention. First, note that the stronger nonlinearity present at the enhancement frequency for the data set II has resulted in splitting into two adjacent enhancement frequencies. This is exemplified in Figure 3 by the response in the radius oscillation at the fundamental frequency. It also occurs in the second, third and fifth harmonics of pressure. A different kind of frequency splitting occurs where a suppression frequency splits into a suppression frequency and an enhancement frequency. This can be seen in the fundamental component of pressure oscillation near the frequency ratio of 1.

Next the effect of varying the void fraction is demonstrated in Figure 4 where data for void fraction values of 0.005, 0.020 and 0.100 are compared. Note that the main features of the results, namely the enhancement and suppression frequencies remain almost the same. However, the nonlinear response is enhanced as the void fraction is reduced. This dependence can be predicted from the linear solution in which both the radius and the pressure are given by terms multiplied by the factor $[(1-\alpha_o)/3\alpha_o]^{1/2}$. The denominator clearly represents the primary influence of void fraction on the results. With increased level of nonlinearity, the frequency splitting phenomena, described earlier, are observed. Also, the first enhancement frequency in the radius oscillations increases slightly with an increased level of nonlinearity. Similarly,the first suppression frequency for pressure oscillations decreases slightly with an increased level of nonlinearity. This also occurs in the higher harmonics.

Finally, the effect of changing the amplitude of the wall motion $X_n(0)/R_o$ for the data set I while keeping the void fraction constant at 0.02 is shown in Figure 5. $X_n(0)/R_o$ values of 0.01, 0.03 and 0.06 are used. Obviously the nonlinear effects become stronger for higher values of $X_n(0)/R_o$. Splitting of some enhancement and suppression frequencies is observed. In addition cancellation of neighbouring suppression and enhancement frequencies can be observed for the fourth harmonic in the radius and pressure oscillations.

6. Conclusions

In this paper we have examined some of the nonlinear effects which can occur when a plane bounding a bubbly liquid oscillates in a direction normal to the plane of the wall. Specifically we have examined the response in terms of the bubble radius oscillations at the wall and the pressure oscillations at the wall. The principal results are as follows. Radius oscillations are dominated by the fundamental response at the bubble natural frequency. On the other hand pressure oscillations at the wall are suppressed near the bubble natural frequency for harmonics of all orders. Pressure oscillations are dominated by fundamental and second harmonic responses at frequencies of approximately $2\omega_b$. It is seen that nonlinear effects are increased as result of a decrease in the surface tension and viscous parameters or a decrease in the void fraction. Nonlinear effects also increase with increase in the amplitude of wall oscillation. Characteristic suppression and enhancement frequencies can be identified and depend upon the level of nonlinearity. Also, increased nonlinearity is manifested in the form of splitting and cancellation of enhancement and suppression frequencies.

7. Acknowledgements

The authors are very grateful for the support of the Office of Naval Research under contract N00014-85-K-0397. We also thank Professors A.J. Acosta and Sheldon Green for their assistance.

8. References

Chahine, G.L. 1982. *Cloud Cavitation : Theory.*, 14th Symp. on Naval Hydrodynamics, Aug 23-27, 1982.

d'Agostino, L., Brennen, C.E. and Acosta, A.J. 1988. *Linearized Dynamics of Two-Dimensional Bubbly and Cavitating Flows Over Slender Surfaces.*, J. Fluid Mechanics, Vol. 192, pp 485-509.

d'Agostino, L. and Brennen, C.E. 1988. *Linearized Dynamics of Spherical Bubble Clouds.* J. Fluid Mechanics, Vol. 199, pp 155-176.

Devin C. Jr. 1959. *Survey of Thermal, Radiation and Viscous Damping of Pulsating Air Bubbles in Water.*, J. Acoustical Soc. of Am., Vol. 31, No. 12, pp 1654-1667.

Eller, A. and Flynn, H.G. 1969. *Generation of Subharmonics of Order One-Half by Bubbles in Sound Field.*, J. Acoustical Soc. of Am., Vol. 46, No.3 (part 2), pp 722-727.

Hansson, I., Kedrinskii, V. and Morch, K.A. 1982. *On the Dynamics of Cavity Clusters.*, J. of Phys., D: Appl. Phys., Vol. 15, pp 1725-1734.

Kumar, S. and Brennen, C.E. 1990. *Nonlinear effects in the dynamics of clouds of bubbles.* Submitted to the J. Acoustical Soc. of Am.

Lauterborn, W. 1976. *Numerical Investigations of Nonlinear Oscillations of Gas Bubbles in Liquids.*, J. Acoustical Soc. of Am., Vol. 59, No. 2, pp 283–293.

Morch, K.A. 1980. *On the collapse of Cavity Clusters in Flow Cavitation.*, In "Cavitation and Inhomogenieties in Underwater Acoustics", ed. W. Lauterborn, Springer Series in Electrophysics, Vol. 4, pp 95–100.

Morch, K.A. 1982. *Energy considerations in the collapse of Cavity Clusters.*, Appl. Sci. Res., Vol. 38, pp 313-321.

Omta, R. 1987. *Oscillations of a Cloud of Bubbles of Small and Not So Small Amplitude.*, J. Acoustical Soc. of Am., Vol. 82 pp 1018–1033.

Plesset, M.S. and Hsieh, D.Y. 1960. *Theory of Gas Bubble Dynamics in Oscillating Pressure Fields.*, Phys. of Fluids, Vol. 3, No. 6, pp 882–892.

Plesset, M. and Prosperetti, A. 1977. *Bubble Dynamics and Cavitation*, Ann. Rev. of Fluid Mech., Vol. 9, pp 145–186.

Prosperetti, A. 1974. *Viscous and Nonlinear Effects in the Oscillations of Drops and Bubbles.*, Ph. D. Thesis, Calif. Inst. of Tech., 1974.

van Wijngaarden, L. 1964. *On the Collective Collapse of Large Number of Gas Bubbles in Water.*, Proc. of 11th Int. Cong. of Appl. Mech., Munich, Germany, 1964, pp 854–861.